

# Effects of dispersion parity-violating interaction in electron scattering and atoms

V. V. Flambaum\* and I. B. Samsonov†

*School of Physics, University of New South Wales, Sydney 2052, Australia*

Exchange of two neutrinos (as well as other fermions) generates a long-range parity-violating (PV) potential of the form  $\sim G^2/r^5$ , with characteristic range  $\hbar/(2m_\nu c)$ . In atomic systems the corresponding matrix elements converge at distances  $r < 10/M_Z$ , so that the interaction between electron and quarks effectively reduces to a contact term  $\sim G^2 M_Z^2 \delta^3(\vec{r}) \sim G \alpha \delta^3(\vec{r})$ . This interaction produces a  $-0.8\%$  correction to the effective weak charge of cesium, resolving the  $2\sigma$  discrepancy between the Standard Model prediction and the measured Cs parity-violation amplitude. The corresponding value of the weak mixing angle is  $\sin^2 \theta_W = 0.2375(19)$  at  $q^2 \approx 0$ , in agreement with the Standard Model prediction  $\sin^2 \theta_W = 0.23873$ . The relative correction to the proton weak charge is about 3%, with a similar correction for the electron weak charge. Using these results, we revisit the limits on an additional  $Z'$  boson and obtain a constraint on isospin-conserving oblique radiative corrections characterized by the Peskin–Takeuchi parameter  $S = -0.32(53)$ , at  $q^2 \approx 0$ .

## I. INTRODUCTION

Exchange of two neutrinos as in Fig. 1 produces long range potential  $\propto G^2/r^5$  in the particle interaction, where  $G$  is the Fermi constant [1–5]. The effects of parity conserving part of this potential are, however, many orders of magnitude smaller than the sensitivity of the experiments [6–13] and are practically unobservable.

In Refs. [14–18] it was noted that the neutrino exchange potential has parity violating (PV) part  $\propto G^2/r^5$  with the range  $\hbar/2m_\nu c$  exceeding atomic size by several orders of magnitude. It was also demonstrated that mixed  $\gamma Z$  electron vacuum polarization produces PV potential  $\propto \alpha G/r^3$  with the range  $\hbar/2m_e c = 193$  fm, which exceeds the range of the weak interaction by five orders of magnitude [14, 16], similar to the range of the Uehling potential due to electron vacuum polarization by the nuclear Coulomb field.

In the present paper we show that the contribution of the diagrams in Fig. 1 with exchange by two neutrinos or by other fermions to the PV effects in atoms is  $\sim 1\%$ , and this significantly exceeds the error 0.35% of the PNC measurement in Cs atom [19] and the error  $< 0.5\%$  in the many-body atomic calculations of the  $Z$ -boson contribution [20–27]. The work is in progress to improve both experimental [28–30] and theoretical [31] accuracy.

The error in atomic calculations cancels out in the ratio of the PV amplitudes in different isotopes of the same atom [32–34]. The measurement for the chain of isotopes of Yb atom was performed in Ref. [35].

The study of PV in atoms provides high precision tests of the Standard Model and new physics beyond it [36, 37].

We will also show that the diagrams on Fig. 1 give significant contributions to the PV effects in low-energy scattering of electron from proton, deuteron and other nuclei. The corresponding corrections to the proton and nuclear weak charges are found. Similar correction to

PV effects in electron-electron (Møller) scattering and electron weak charge is expected.

Weak charge  $Q_W$  is the constant of the electron-nucleon weak interaction due to the  $Z$ -boson exchange which has interaction range  $r_Z = \hbar/M_Z c \approx 0.002$  fm. On the nuclear and atomic scales this may be considered as a Fermi-type contact interaction.

Radiative corrections to the proton and neutron weak charges of the order  $\alpha \approx 1/137$  have been calculated in Refs. [38–42] and were shown to exceed 1%. However, diagrams on Fig. 1, which actually give comparable contributions, have not been included into these calculations. The point is that at large distance these diagrams give interaction proportional to  $G^2$ , which is very small. However, this interaction is highly singular,  $\propto G^2/r^5$ , and integration over distance with electron wave functions and effective cut-off at  $r \sim 1/M_Z$  gives contribution  $\sim G^2 M_Z^2 \sim \alpha G$ . Thus, the suppression relative to the ordinary weak interaction mediated by the  $Z$ -boson exchange is  $\sim \alpha$  [16].

For electron-electron scattering there are also box diagrams with crossing electron and crossing neutrinos lines. Note that in the case of Majorana neutrinos, there is an additional box diagram with neutrinos as the vertical sides. Potentially, this could give a possibility to identify Majorana neutrinos using PV in electron scattering, but the contribution of this diagram is small.

To perform accurate calculations, we require the effective potential generated by the diagrams shown in Fig. 1 at distances  $r \sim 1/M_Z$ . The neutrino-exchange contribution to this potential, valid for all distances satisfying  $r \ll 1/m_\nu$ , was calculated in Refs. [17, 18], and our analysis is based on these results. We further include the additional contributions arising from other fermions in the loop.

In this paper, we use natural units with  $\hbar = c = 1$ .

\* v.flambaum@unsw.edu.au

† igor.samsonov@unsw.edu.au

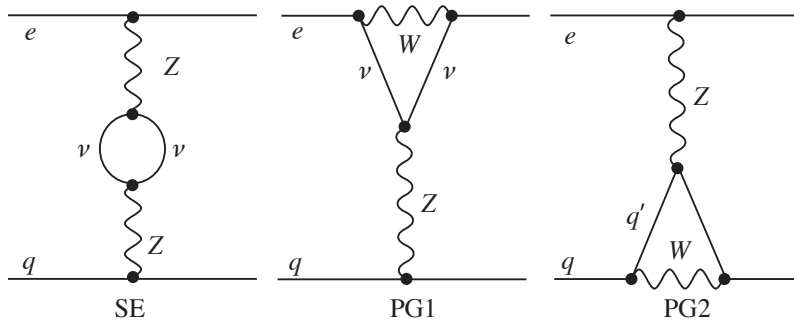


FIG. 1. Feynman diagrams contributing to the long-range force due to neutrino exchange between electron  $e$  and quark  $q$ . The self-energy (SE) diagram may also contain other leptons and quarks in the loop while the ‘penguin’ (PG1) diagram has only the electronic neutrino in the loop.

## II. EFFECTIVE POTENTIAL DUE TO THE FERMION LOOP

Parity violating interactions produce PV effects in atoms by mixing  $s_{1/2}$  and  $p_{1/2}$  electron orbitals. To find corrections produced by diagrams on Fig. 1 it is sufficient to calculate the ratio of the matrix elements

$$\frac{\langle ns_{1/2}|W_f(r)|n'p_{1/2}\rangle}{\langle ns_{1/2}|W_Z(r)|n'p_{1/2}\rangle}, \quad (1)$$

where  $W_Z$  and  $W_f$  are the PV potentials produced by  $Z$  boson tree-level exchange and  $f$  fermion loop correspondingly.

Dominating contribution to both matrix elements comes from the distance between electron and quark of order  $r \sim 1/M_Z$ , which is very small as compared to the scale of the variation of electron wave functions and nuclear size. Therefore, we may replace both potentials by their Fermi-type contact approximations  $w_{Z,f}\delta^3(\vec{r})$  using relation  $\int W_{Z,f}(r)4\pi r^2 dr = w_{Z,f} \int \delta^3(\vec{r})d^3r$ . Then the nuclear-spin-independent (NSI) part of the electron-nucleus PV operator  $W(r)$  may be cast in the form

$$W(r) = -\frac{G}{2\sqrt{2}}(Q_W + \delta Q_W)\gamma_5\rho(r), \quad (2)$$

where  $Q_W = -N + (1 - 4\sin^2\theta_W)Z$  is the weak nuclear charge,  $\delta Q_W$  is the correction produced by the diagrams on Fig. 1,  $\rho(r)$  is the nuclear density normalized by the condition  $\int \rho(r)d^3r = 1$ ,  $N$  and  $Z$  are numbers of neutrons and protons in the nucleus, respectively. Inclusion of radiative corrections gives [43, 44]

$$\begin{aligned} Q_W &= -0.98897N + (1.0250 - 3.9978\sin^2\theta_W)Z \\ &= -0.98897N + 0.070605Z. \end{aligned} \quad (3)$$

For cesium atom, this formula implies the standard model value of the weak charge  $Q_W^{SM} = -73.26(1)$  assuming  $\sin^2\theta_W = 0.23873$  at zero momentum transfer [44]. The experimental measurements of the parity violation in cesium atom give  $\sin^2\theta_W = 0.2349(18)$  at  $q = 2.4$  MeV [44].

Note that the differences in the experimental values of Cs weak charge and Weinberg angle in 2024 and 2022 editions of Particle Data group reviews are due to the different values of the Stark polarizability  $\beta$  used (Cs PV experiment measures ratio of the PV amplitude to  $\beta$ ). The 2023 paper [45] corrected the result of Ref. [46] and confirmed the original value of  $\beta$  found in our paper [47].

Calculations of the neutrino exchange potentials, presented in Appendix, are similar to that described in detail in Ref. [17]. Let us start from the self-energy (SE) diagram in Fig. 1. The interaction constant on the bottom fermion line cancels with the single  $Z$ -boson exchange contribution in the ratio (1). Therefore, for any fermion on the bottom line (e.g. quark or electron in the electron-electron scattering case) the ratio of the SE diagram to the tree-level  $Z$ -boson contribution is the same. As a result we obtain

$$\frac{\delta Q_W^{(SE)}}{Q_W} = -\frac{g^2}{96\pi^2 c_W^2} N_{\text{eff}} = -0.86\%, \quad (4)$$

where  $g \approx 0.65$  is the  $Z$ -boson-neutrino interaction constant,  $c_W^2 = 1 - s_W^2 = 0.76127$ ,  $s_W^2 \equiv \sin^2\theta_W$ . Following Refs. [11, 16], we introduced here effective number of neutrinos,

$$N_{\text{eff}} \approx 14.5. \quad (5)$$

Indeed, there are 3 ordinary neutrinos. However, we should add one-loop contributions of all fermions with masses smaller than that of the  $Z$ -boson, including  $e, \mu, \tau, u, d, s, c, b$ .  $N_{\text{eff}}$  is not an integer number since interaction constants of other fermions with  $Z$ -boson are different from that for neutrinos, see Appendix B 1.

Diagrams PG1 and PG2 in Fig. 1 do not have enhancement factor  $N_{\text{eff}}$ . Using the calculations of the momentum and radial integrals presented in Appendix A 2 with the result in Eq. (A23), we obtain the following correction to the nuclear weak charge (see also Appendix B 3 for details):

$$\frac{\delta Q_W^{(PG)}}{Q_W} = 1.7 \times 10^{-3} \frac{N - Z}{N - (1 - 4s_W^2)Z}, \quad (6)$$

For the proton weak charge this ratio, enhanced by the small value of  $(1 - 4 \sin^2 \theta_W) = 0.044$  in the denominator, is 3.8%. Adding contribution (4) corresponding to the SE diagram, we obtain the total correction to the nuclear weak charge

$$\frac{\delta Q_W}{Q_W} = \left( -0.86 + 0.17 \frac{N - Z}{N - (1 - 4s_W^2)Z} \right) \%. \quad (7)$$

Equation (7) shows that the contribution of the diagrams PG1 and PG2 (given in the last term) for all atoms, except for hydrogen, is small, so we obtain  $\delta Q_W/Q_W \approx -0.8\%$  in all medium and heavy atoms. For the proton weak charge this gives,

$$\frac{\delta q_W^p}{q_W^p} \approx 3.0\%. \quad (8)$$

Similar relative correction to the PV effect in muonium atom was obtained in Refs. [17, 18], where the authors do not interpret this as a correction to the weak charge. The enhancement due to the small value of  $(1 - 4s_W^2)$  in denominator is also expected for the electron weak charge in the case of PV in electron-electron Møller scattering.

Distribution of proton and neutron densities in the nucleus are slightly different. Therefore to take into account this effect in numerical calculations it may be convenient to separate proton and neutron contributions to the weak charge. Adding the corrections (7) to Eq. (3) we find

$$\begin{aligned} Q_W + \delta Q_W &= -0.98207N + (1.0181 - 3.9634s_W^2)Z \\ &= -0.98207N + 0.071918Z. \end{aligned} \quad (9)$$

Here we assume the SM value of the Weinberg angle with  $\sin^2 \theta_W = 0.23873$  at zero momentum transfer [44].

### III. COMPARISON WITH EXPERIMENTAL DATA ON WEAK CHARGES AND LIMITS ON NEW PHYSICS

If we use the value of the proton weak charge obtained in the recent very accurate lattice calculation [48],  $Q_W^{SM} = 0.06987(50)$ , we obtain corrected value  $Q_W^{SM} + \delta Q_W^{SM} = 0.06987(1 + 0.03) = 0.0719$ . It agrees with  $Q_W^{\text{exp}} = 0.0719(45)$  measured by Qweak collaboration [49].

The correction to the electron weak charge is also expected at the level of several per cent. This does not contradict to the experimental value of the electron weak charge  $Q_W^{\text{exp}} = -0.053(11)$  obtained by E158 collaboration [50]. The accuracy in the experimental measurement of the proton weak charge in the electron-proton scattering by the Qweak collaboration is 7%, the accuracy in the measurement of the PV asymmetry in electron-electron scattering by E158 collaboration is 20%. However, both experimental collaborations are expecting significant improvements of the accuracy soon.

The most sensitive point to the weak charge correction is currently in cesium PV experiments, where

$\delta Q_W/Q_W \approx -0.8\%$  exceeds both the experimental error 0.35% and the error in our atomic many-body calculation which is under 0.5%. This correction actually eliminates  $2\sigma$  difference between the measured  $Q_W^{\text{exp}} = -72.41(42)$  and the standard model  $Q_W^{SM} + \delta Q_W^{SM} = -73.26(1 - 0.008) = -72.67$  weak charges.

After including  $\delta Q_W^{SM}$ , the measured in Cs PV experiment value of the Weinberg angle at  $q^2 \approx 0$ ,

$$\sin^2 \theta_W = 0.2375(19), \quad (10)$$

also comes to a perfect agreement with prediction of the standard model  $\sin^2 \theta_W = 0.2387$ .

The difference  $Q_W^{\text{exp}} - (Q_W^{SM} + \delta Q_W^{SM}) = 0.26(42)$  allows us to obtain limits on new physics. The limits on the additional  $Z'$ -boson interaction strength obtained as a function of  $Z'$  mass from the measurements of PV in Cs atom are approximately 2 times stronger than that presented in Table II and Fig. 1 of Ref. [51]. For  $m_{Z'} \gg \alpha Z m_e$ , the products of  $Z'$  interaction constants with the electron and nucleus obeys the following bound:  $|g_e^A g_N^V|/m_{Z'}^2 < 2.2 \times 10^{-8} \text{ GeV}^{-2}$ . For  $m_{Z'} \ll 1/R_{\text{atom}}$ , the product of these constants is limited by  $|g_e^A g_N^V| < 1.7 \times 10^{-14}$ .

We also obtain limits on oblique radiative corrections produced by new particles. Ref. [52] calculated the shift of the weak charge produced by these corrections  $\Delta Q_W = -0.8S$ , where  $S$  is the Peskin–Takeuchi parameter characterizing isospin-conserving vacuum-polarization effects. Comparing this expression with the measured value  $\Delta Q_W = 0.26(42)$ , we obtain

$$S = -0.32(53). \quad (11)$$

The global electroweak fit of  $S$  [44] is dominated by the  $Z$ -pole and  $W$ -mass measurements, while atomic PV probes oblique radiative corrections at very low momentum transfer,  $q^2 \approx 0$ , thereby testing their running over a wide range of scales. Light weakly interacting states can induce momentum-dependent vacuum-polarization effects that contribute differently at  $q^2 \approx 0$  and  $q^2 \sim m_Z^2$ . In this case, PV in cesium provides sensitivity to new physics effects that may not be fully captured by high-energy fits.

*Acknowledgments.* – The work was supported by the Australian Research Council Grant No. DP230101058.

#### Appendix A: Reduction of effective interaction potentials to the contact interaction

The exchange of various SM particles other than photon between two point-like fermions may be described by potential forces which may be considered as a perturbation to the Coulomb interaction potential. If such a potential  $V(r)$  is short-range as compared with the size of the nucleus, they may be effectively reduced to the contact interaction with the the delta-function potential,

$$V_{\text{contact}}(\vec{r}) = \kappa \delta^3(\vec{r}), \quad (A1)$$

with some coefficient  $\kappa$  defined by

$$\kappa = \int V(r) d^3r. \quad (\text{A2})$$

The canonical example is the exchange of the  $Z$  boson which is described by the potential

$$V_Z(r) = -\frac{g^2}{64\pi c_W^2} \frac{e^{-m_Z r}}{r}, \quad (\text{A3})$$

where  $g \approx 0.65$  is the gauge coupling constant of the  $SU(2)_L$  group, and  $c_W \equiv \cos\theta_W \approx 0.87$  is the cos of Weinberg angle. We omit here Dirac matrix  $\gamma_5$ , see Eq. (2). Since the range of this interaction is  $r = O(m_Z^{-1})$ , in atomic calculations it may be replaced with the contact interaction (A1) with the coefficient

$$\kappa_Z = -\frac{g^2}{16c_W^2 m_Z^2}. \quad (\text{A4})$$

Below, we consider effective potentials corresponding to the exchange of neutrinos as per the Feynman graphs in Fig. 1. In the present work, we need two such potentials, which are usually referred to as the self-energy (SE) and ‘penguin’ (PG) contributions, respectively. These potentials were found in the works [17, 18]. We will calculate the corresponding contact interaction coefficients  $\kappa$  for these potentials.

### 1. Neutrino self-energy diagram

The potential corresponding to the massless neutrino one-loop self-energy diagram was calculated in Refs. [17, 18]:

$$V_{\text{SE}}(r) = -V_{0,\text{SE}} \frac{1}{r} \int_0^\infty dt \frac{t e^{-r\sqrt{t}}}{(t - m_Z^2)^2}, \quad (\text{A5})$$

where

$$V_{0,\text{SE}} = \frac{g^4}{(4c_W)^4} \frac{1}{24\pi^3}. \quad (\text{A6})$$

The integral in Eq. (A5) is divergent because of the double pole in the denominator. This double pole is regularized by a small shift along the imaginary axis, and by retaining the principal value of the integral [17]. As a result, one finds

$$V_{\text{SE}}(r) = \frac{V_0}{2r} \left[ e^{m_Z r} (2 + m_Z r) \text{Ei}(-m_Z r) + e^{-m_Z r} (2 - m_Z r) \text{Ei}(m_Z r) + 2 \right], \quad (\text{A7})$$

where

$$\text{Ei}(x) \equiv -\int_{-x}^\infty t^{-1} e^{-t} dt. \quad (\text{A8})$$

The asymptotic behavior of the potential (A7) is

$$V(r)|_{r \gg m_Z^{-1}} = -\frac{g^4}{2\pi^3 c_W^4 r^5}. \quad (\text{A9})$$

This potential plays significant role at the distance  $r \sim m_Z^{-1}$ , and decays rapidly at  $r \gg m_Z^{-1}$ . Hence, in atomic calculations, this potential may be replaced with the contact interaction potential (A1) where the coefficient  $\kappa$  is found to be

$$\kappa_{\text{SE}} = 4\pi \int_0^\infty r^2 V(r) dr = \frac{4\pi V_{0,\text{SE}}}{m_Z^2}. \quad (\text{A10})$$

Here the following identity was used:

$$\int_0^\infty [e^x(2+x)\text{Ei}(-x) + e^{-x}(2-x)\text{Ei}(x) + 2] x dx = 2. \quad (\text{A11})$$

Comparing Eq. (A10) with Eq. (A4) we find

$$\frac{\kappa_{\text{SE}}}{\kappa_Z} = -\frac{g^2}{96\pi^2 c_W^2} \approx -5.9 \times 10^{-4}. \quad (\text{A12})$$

### 2. Triangle PG diagram contribution to the potential

The contribution to the potential from the triangle PG diagrams was found in Refs. [17, 18] in the following form:

$$V_{\text{PG}}(r) = -V_{0,\text{PG}} \frac{1}{r} \text{Re}I(r), \quad (\text{A13a})$$

$$I(r) = \int_0^\infty dt e^{-\sqrt{t}r} \times \frac{t(2m_W^2 + 3t) - 2(m_W^2 + t)^2 \ln\left(1 + \frac{t}{m_W^2}\right)}{t^2(t - m_Z^2 + i0)}, \quad (\text{A13b})$$

where

$$V_{0,\text{PG}} = \frac{g^4}{2048\pi^3 c_W^2}. \quad (\text{A14})$$

Here the principal value of the integral is assumed near the pole  $t = m_Z^2$ . In Ref. [17], it was shown that the potential (A13) possesses the following asymptotic behavior

$$V_{\text{PG}}(r)|_{r \gg m_Z^{-1}} = -\frac{g^4}{256\pi^3 c_W^2 m_Z^2 m_W^2 r^5}. \quad (\text{A15})$$

Thus, this potential drops rapidly and its effects become negligible at the distance of a few  $m_Z^{-1}$ . In atomic calculations, within the current accuracy goal the potential corresponding to the PG diagram may be replaced by the contact interaction (A1) with the corresponding coefficient  $\kappa$ .

To compare the potential (A13a) with contact interaction (A1), we need to calculate the coefficient

$$\kappa_{\text{PG}} = -4\pi V_{0,\text{PG}} \int_0^\infty I(r) r dr. \quad (\text{A16})$$

Substituting here Eq. (A13b) and integrating over  $r$ , we find

$$I_0 \equiv \int_0^\infty I(r)r dr = \frac{1}{m_W^2} \int_0^\infty \frac{x(2+3x) - 2(1+x)^2 \ln(1+x)}{x^3(x-z)} dx. \quad (\text{A17})$$

where  $z \equiv \frac{m_\tau^2}{m_W^2}$ . Making use of the identity

$$\ln(1+x) = x^2 - \frac{x^2}{2} + x^3 \int_0^1 \frac{\alpha^2 d\alpha}{1+\alpha x}, \quad (\text{A18})$$

reduces the problem to the integration of rational functions,

$$I_0 = \frac{1}{m_W^2} \int_0^\infty \frac{xdx}{x-z} - \frac{2}{m_W^2} \int_0^1 \alpha^2 d\alpha \int_0^\infty \frac{(1+x)^2 dx}{(1+\alpha x)(x-z)}. \quad (\text{A19})$$

It is possible to show that all divergent terms in these integrals cancel, and the finite result is

$$I_0 = \frac{1}{2z^3 m_W^2} \left[ 4(z+1)^2 \text{Li}_2(-z) + 4(z+1)^2 \ln(z) \ln(z+1) + z(7z-2(3z+2) \ln(z)+4) \right]. \quad (\text{A20})$$

Recalling that  $z = c_W^{-2}$ , we find

$$I_0 = \frac{1}{2m_Z^2} \left[ 4(c_W^2 + 1)^2 \text{Li}_2(-c_W^{-2}) + 4c_W^2 - 2 \log(c_W) (-4c_W^2 + 4(c_W^2 + 1)^2 \log(c_W^{-2} + 1) - 6) + 7 \right] \approx -\frac{0.92}{m_Z^2}. \quad (\text{A21})$$

As a result, the coefficient (A16) is found to be:

$$\kappa_{\text{PG}} \approx 15V_{0,\text{PG}} m_Z^{-2} \approx 5.4 \times 10^{-5} m_Z^{-2}. \quad (\text{A22})$$

Comparing this coefficient with Eq. (A4), we find

$$\frac{\kappa_{\text{PG}}}{\kappa_Z} \approx -1.6 \times 10^{-3}. \quad (\text{A23})$$

## Appendix B: Calculation of vertex constant prefactor

In this paper, we study long-range forces between electron and nucleon with the range  $r \gg O(m_Z^{-1})$ . This interaction is mediated by SM particles with masses  $m \ll m_Z$ , which are  $\nu^\alpha = (\nu_e, \nu_\mu, \nu_\tau)$  for neutrinos,  $l^\alpha = (e, \mu, \tau)$

	$c_V$	$c_A$
$l^\alpha$	$4s_W^2 - 1$	-1
$u, c, t$	$1 - \frac{8}{3}s_W^2$	1
$d, s, b$	$\frac{4}{3}s_W^2 - 1$	-1
$p$	$1 - 4s_W^2$	1
$n$	-1	-1

TABLE I. Values of the vector  $c_V$  and axial-vector  $c_A$  interaction constants for leptons  $l^\alpha = (e, \mu, \tau)$ , quarks, proton  $p$  and neutron  $n$ .  $s_W^2 = \sin^2 \theta_W$ , where  $\theta_W$  is the Weinberg angle.

for electron, muon and tau,  $q_k = (u, d, s, c, b)$  for quarks. The relevant part of the SM Lagrangian is

$$\begin{aligned} \mathcal{L} = & \frac{g}{4c_W} [\bar{\nu}^\alpha \gamma^\mu (1 - \gamma_5) \nu^\alpha + \bar{l}^\alpha \gamma^\mu (c_V^\alpha - c_A^\alpha \gamma_5) l^\alpha \\ & + \bar{q}_k \gamma^\mu (c_V^{q_k} - c_A^{q_k} \gamma_5) q_k] Z_\mu \\ & + \frac{g}{2\sqrt{2}} [\bar{l}^\alpha \gamma^\mu (1 - \gamma_5) \nu^\alpha W_\mu^- \\ & + \bar{u} \gamma^\mu (1 - \gamma_5) d W_\mu^+ + h.c.] \end{aligned} \quad (\text{B1})$$

Here we ignore the the CKM matrix because the quarks in the loop may be effectively considered as massless.

The values of the vector and axial-vector constants are given in Table I.

### 1. Electron-proton effective interaction

At high momentum transfer, the proton is represented by three valence quarks  $p = uud$ . In the tree-level diagram,  $Z$  boson interacts with each of these quarks, thus,  $c_V^p = 2c_V^u + c_V^d = 1 - 4s_W^2$ . Hence, the tree-level  $Z$ -boson exchange diagram contains the following combination of wave functions

$$\begin{aligned} & [\bar{e} \gamma^\mu (c_V^e - c_A^e \gamma_5) e] [\bar{p} \gamma_\mu (c_V^p - c_A^p \gamma_5) p] \\ & = -c_A^e c_V^p [\bar{e} \gamma^\mu \gamma_5 e] [\bar{p} \gamma_\mu p] + \dots, \end{aligned} \quad (\text{B2})$$

and the corresponding prefactor is

$$-c_A^e c_V^p = 1 - 4s_W^2. \quad (\text{B3})$$

The same prefactor appears in the SE diagram in Fig 1. Therefore, these vertex constants cancel out in the ratio of matrix elements (1).

The SE diagram is, however, enhanced by the factor (5). In addition to the three neutrinos, this factor receives the following contributions. There are three left leptons with the  $Z$ -boson interaction constant  $\frac{1}{2}(c_V^l + c_A^l) = 2s_W^2 - 1$ , and three right leptons with vertex constants  $\frac{1}{2}(c_V^l - c_A^l) = 2s_W^2$ . Then there are  $2 \times 3$  ( $u$  and  $c$  quarks with three colors) left up-like quarks with the  $Z$ -boson interaction constants  $\frac{1}{2}(c_V^u + c_A^u) = 1 - \frac{4}{3}s_W^2$ , and the same number of the corresponding right quarks with the vertex constants  $\frac{1}{2}(c_V^u - c_A^u) = -\frac{4}{3}s_W^2$ . Finally, there are  $3 \times 3$  ( $d, s, b$  with three colors) right down-like quarks

with the vertex constant  $\frac{1}{2}(c_V^d + c_A^d) = \frac{2}{3}s_W^2 - 1$ , and the same number of the corresponding right quarks with the constant  $\frac{1}{2}(c_V^d - c_A^d) = \frac{2}{3}s_W^2$ . All these coefficients enter the SE diagram in Fig. 1 quadratically. Combining them we find

$$N_{\text{eff}} = \frac{160}{3}s_W^4 - 40s_W^2 + 21 \approx 14.5. \quad (\text{B4})$$

This explains the coefficients in Eq. (4).

The PG1 diagram in Fig. 1 has loop on the electron line, and  $Z$ -boson interacts with the proton line which consists of the three valence quarks. Therefore, this diagram contains the following combination of the wave functions (see also Appendix A in Ref. [17]):

$$[\bar{e}\gamma^\mu(1-\gamma_5)e][\bar{p}\gamma_\mu(c_V^p - c_A^p\gamma_5)p] = -c_V^p[\bar{e}\gamma^\mu\gamma_5e][\bar{p}\gamma_\mu p] + \dots \quad (\text{B5})$$

There are three PG2 diagrams with the loop on the quark lines: two diagrams with  $u \rightarrow d + W^+$ , and one diagram with  $d \rightarrow u + W^-$ . These diagrams contain the following combinations of wave functions:

$$[\bar{e}\gamma^\mu(-\gamma_5c_A^e)e][\bar{d}\gamma_\mu c_V^u d] = -c_A^e c_V^u [\bar{e}\gamma^\mu\gamma_5e][\bar{d}\gamma_\mu d] \quad (\text{B6})$$

$$[\bar{e}\gamma^\mu(-\gamma_5c_A^e)e][\bar{u}\gamma_\mu c_V^d u] = -c_A^e c_V^d [\bar{e}\gamma^\mu\gamma_5e][\bar{u}\gamma_\mu u]. \quad (\text{B7})$$

The combined prefactor is

$$-c_V^p - 2c_A^e c_V^d - c_A^e c_V^u = 4s_W^2 - 1 - 1 = -2 + 4s_W^2. \quad (\text{B8})$$

The ratio of prefactors (B8) and (B3) is

$$-\frac{2 - 4s_W^2}{1 - 4s_W^2} \approx -23. \quad (\text{B9})$$

The corresponding relative correction to the proton weak charge is the product of Eqs. (A23) and (B9):

$$\frac{\delta Q_p}{Q_p} = -\frac{2 - 4s_W^2}{1 - 4s_W^2} \frac{\kappa_{\text{PG}}}{\kappa_Z} \approx \frac{1.7 \times 10^{-3}}{1 - 4s_W^2}. \quad (\text{B10})$$

## 2. Electron-neutron effective interaction

Neutron is represented by the three valence quarks,  $n = udd$ . The corresponding  $Z$ -boson vector coupling is  $c_V^n = c_V^u + 2c_V^d = -1$ . Therefore, tree-level  $Z$ -boson exchange diagram has the prefactor

$$-c_A^e c_V^n = -1. \quad (\text{B11})$$

The same prefactor appears in the SE diagram, which is enhanced by the effective number of neutrinos (5).

In the PG1 diagram, there is the following combination of wave functions:

$$[\bar{e}\gamma^\mu(1-\gamma_5)e][\bar{n}\gamma_\mu(c_V^n - c_A^n\gamma_5)n] = -c_V^n[\bar{e}\gamma^\mu\gamma_5e][\bar{n}\gamma_\mu n] + \dots \quad (\text{B12})$$

There are also three PG2 diagrams: one diagram with  $u \rightarrow d + W^+$ , and two with  $d \rightarrow u + W^-$ . These diagrams contain the following combinations of wave functions:

$$[\bar{e}\gamma^\mu(-\gamma_5c_A^e)e][\bar{u}\gamma_\mu c_V^d u] = -c_A^e c_V^d [\bar{e}\gamma^\mu\gamma_5e][\bar{u}\gamma_\mu u] \quad (\text{B13})$$

$$[\bar{e}\gamma^\mu(-\gamma_5c_A^e)e][\bar{d}\gamma_\mu c_V^u d] = -c_A^e c_V^u [\bar{e}\gamma^\mu\gamma_5e][\bar{d}\gamma_\mu d]. \quad (\text{B14})$$

The combined prefactor is

$$-c_V^n - c_A^e c_V^d - 2c_A^e c_V^u = 2 - 4s_W^2. \quad (\text{B15})$$

The ratio of prefactors (B15) and (B11) is

$$\frac{2 - 4s_W^2}{-1} = -(2 - 4s_W^2). \quad (\text{B16})$$

The corresponding relative correction to the neutron weak charge is the product of Eqs. (A23) and (B16):

$$\frac{\delta Q_n}{Q_n} = -(2 - 4s_W^2) \frac{\kappa_{\text{PG}}}{\kappa_Z} \approx 1.7 \times 10^{-3}. \quad (\text{B17})$$

## 3. Contribution to the nuclear weak charge due to PG diagrams

Combination of Eqs. (B10) and (B17) gives us the correction to the weak charge of a nucleus composed of  $Z$  protons and  $N$  neutrons due to the PG diagrams,

$$\delta Q^{(\text{PG})} \approx \frac{1.7 \times 10^{-3}}{1 - 4s_W^2} Z \cdot Q_p + 1.7 \times 10^{-3} N \cdot Q_n, \quad (\text{B18})$$

and substituting here tree-level weak charges  $Q_p = 1 - 4s_W^2$  and  $Q_n = -1$ , we have

$$\delta Q^{(\text{PG})} \approx 1.7 \times 10^{-3} (Z - N). \quad (\text{B19})$$

Dividing this expression by the tree-level value of the nuclear weak charge,  $Q_W = -N + (1 - 4s_W^2)Z$ , we obtain the contribution (6).

- 
- [1] Tamm I., Interaction of neutrons and protons, *Nature* **134**, 1010 (1934).  
 [2] R. P. Feynman, *Feynman Lectures on Gravitation*, edited by F. B. Morinigo, W. G. Wagner, and B. Hatfield (Addison-Wesley, Reading, MA, 1996).

- [3] G. Feinberg and J. Sucher, Long-range forces from neutrino-pair exchange, *Phys. Rev.* **166**, 1638 (1968).  
 [4] G. Feinberg, J. Sucher, and C.-K. Au, The dispersion theory of dispersion forces, *Phys. Rep.* **180**, 83 (1989).  
 [5] S. D. H. Hsu and P. Sikivie, Long-range forces from two-neutrino exchange reexamined, *Phys. Rev. D* **49**, 4951

- (1994).
- [6] D. J. Kapner, T. S. Cook, E. G. Adelberger, J. H. Gundlach, B. R. Heckel, C. D. Hoyle, and H. E. Swanson, Tests of the gravitational inverse-square law below the dark-energy length scale, *Phys. Rev. Lett.* **98**, 021101 (2007), [arXiv:hep-ph/0611184](#).
- [7] E. G. Adelberger, B. R. Heckel, S. A. Hoedl, C. D. Hoyle, D. J. Kapner, and A. Upadhye, Particle physics implications of a recent test of the gravitational inverse square law, *Phys. Rev. Lett.* **98**, 131104 (2007), [arXiv:hep-ph/0611223](#).
- [8] Y. J. Chen, W. K. Tham, D. E. Krause, D. Lopez, E. Fischbach, and R. S. Decca, Stronger limits on hypothetical Yukawa interactions in the 30–8000 nm range, *Phys. Rev. Lett.* **116**, 221102 (2016), [arXiv:1410.7267 \[hep-ex\]](#).
- [9] G. Vasilakis, J. M. Brown, T. W. Kornack, and M. V. Romalis, Limits on new long range nuclear spin-dependent forces set with a  $K^{-3}He$  comagnetometer, *Phys. Rev. Lett.* **103**, 261801 (2009), [arXiv:0809.4700 \[physics.atom-ph\]](#).
- [10] W. A. Terrano, E. G. Adelberger, J. G. Lee, and B. R. Heckel, Short-range spin-dependent interactions of electrons: a probe for exotic pseudo-Goldstone bosons, *Phys. Rev. Lett.* **115**, 201801 (2015), [arXiv:1508.02463 \[hep-ex\]](#).
- [11] Y. V. Stadnik, Probing long-range neutrino-mediated forces with atomic and nuclear spectroscopy, *Phys. Rev. Lett.* **120**, 223202 (2018).
- [12] Y. V. Stadnik, V. V. Dzuba, V. V. Flambaum, and P. Munro-Laylim, Errata: Probing long-range neutrino-mediated forces with atomic and nuclear spectroscopy, *Phys. Rev. Lett.* **129**, 239901 (2022).
- [13] P. Munro-Laylim, V. Dzuba, and V. Flambaum, Effects of the long-range neutrino-mediated force in atomic phenomena, *Mol. Phys.* **121**, e2160385 (2023).
- [14] V. V. Flambaum and E. V. Shuryak, Influence of Meson’s Widths on Yukawa-like Potentials and Lattice Correlation Functions, *Phys. Rev. C* **76**, 065206 (2007), [arXiv:nucl-th/0702038](#).
- [15] M. Ghosh, Y. Grossman, and W. Tangarife, Probing the two-neutrino exchange force using atomic parity violation, *Phys. Rev. D* **101**, 116006 (2020), [arXiv:1912.09444 \[hep-ph\]](#).
- [16] V. A. Dzuba, V. V. Flambaum, and P. Munro-Laylim, Long-range parity-nonconserving electron-nucleon interaction, *Phys. Rev. A* **106**, 012817 (2022), [arXiv:2205.02569 \[hep-ph\]](#).
- [17] M. Ghosh, Y. Grossman, C. Sieng, and B. Yu, Neutrino force at all length scales, *Phys. Rev. D* **112**, 113004 (2025), [arXiv:2410.19059 \[hep-ph\]](#).
- [18] M. Ghosh, Y. Grossman, C. Sieng, and B. Yu, Neutrino effects on atomic measurements of the Weinberg angle, *Phys. Rev. Lett.* **135**, 251803 (2025), [arXiv:2512.07938 \[hep-ph\]](#).
- [19] C. S. Wood, S. C. Bennett, D. Cho, B. P. Masterson, J. L. Roberts, C. E. Tanner, and C. E. Wieman, Measurement of parity nonconservation and an anapole moment in cesium, *Science* **275**, 1759 (1997).
- [20] V. A. Dzuba, V. V. Flambaum, and O. P. Sushkov, Summation of the high orders of perturbation theory for the parity nonconserving E1 amplitude of 6s-7s transition in cesium atom, *Phys. Lett. A* **141**, 147 (1989).
- [21] V. A. Dzuba, V. V. Flambaum, and J. S. M. Ginges, High-precision calculation of parity nonconservation in cesium and test of the standard model, *Phys. Rev. D* **66**, 076013 (2002), [arXiv:hep-ph/0204134](#).
- [22] S. A. Blundell, W. R. Johnson, and J. Sapirstein, High accuracy calculation of the  $6s_{1/2} \rightarrow 7s_{1/2}$  parity nonconserving transition in atomic cesium and implications for the standard model, *Phys. Rev. Lett.* **65**, 1411 (1990).
- [23] S. A. Blundell, J. R. Sapirstein, and W. R. Johnson, High accuracy calculation of parity nonconservation in cesium and implications for particle physics, *Phys. Rev. D* **45**, 1602 (1992).
- [24] V. V. Flambaum and J. S. M. Ginges, The radiative potential method for calculations of QED radiative corrections to energy levels and electromagnetic amplitudes in many-electron atoms, *Phys. Rev. A* **72**, 052115 (2005), [arXiv:physics/0507067](#).
- [25] S. G. Porsev, K. Beloy, and A. Derevianko, Precision determination of electroweak coupling from atomic parity violation and implications for particle physics, *Phys. Rev. Lett.* **102**, 181601 (2009), [arXiv:0902.0335 \[hep-ph\]](#).
- [26] S. G. Porsev, K. Beloy, and A. Derevianko, Precision determination of weak charge of  $^{133}Cs$  from atomic parity violation, *Phys. Rev. D* **82**, 036008 (2010), [arXiv:1006.4193 \[hep-ph\]](#).
- [27] V. A. Dzuba, J. C. Berengut, V. V. Flambaum, and B. Roberts, Revisiting parity non-conservation in cesium, *Phys. Rev. Lett.* **109**, 203003 (2012), [arXiv:1207.5864 \[hep-ph\]](#).
- [28] A. Damitz, G. Toh, E. Putney, C. E. Tanner, and D. S. Elliott, Measurement of the radial matrix elements for the  $6s\ ^2S_{1/2} \rightarrow 7p\ ^2P_J$  transitions in cesium, *Phys. Rev. A* **99**, 062510 (2019), [arXiv:1904.06362 \[physics.atom-ph\]](#).
- [29] G. Toh, A. Damitz, N. Glotzbach, J. Quirk, I. C. Stevenson, J. Choi, M. S. Safronova, and D. S. Elliott, Electric dipole matrix elements for the  $6p\ ^2P_J \rightarrow 7s\ ^2S_{1/2}$  transition in atomic cesium, *Phys. Rev. A* **99**, 032504 (2019), [arXiv:1901.00480 \[physics.atom-ph\]](#).
- [30] J. A. Quirk, L. Sherman, A. Damitz, C. E. Tanner, and D. S. Elliott, Measurement of the hyperfine coupling constants and absolute energies of the  $12s\ ^2S_{1/2}$ ,  $13s\ ^2S_{1/2}$ , and  $11d\ ^2D_J$  levels in atomic cesium, *Phys. Rev. A* **105**, 022819 (2022), [arXiv:2201.00755 \[physics.atom-ph\]](#).
- [31] H. B. T. Tan, D. Xiao, and A. Derevianko, Parity-mixed coupled-cluster formalism for computing parity-violating amplitudes, *Phys. Rev. A* **105**, 022803 (2022), [arXiv:2112.04059 \[physics.atom-ph\]](#).
- [32] V. A. Dzuba, V. V. Flambaum, and I. B. Khriplovich, Enhancement of  $P$ - and  $T$ -nonconserving effects in rare-earth atoms, *Z. Phys. D* **1**, 243 (1986).
- [33] B. A. Brown, A. Derevianko, and V. V. Flambaum, Calculations of the neutron skin and its effect in atomic parity violation, *Phys. Rev. C* **79**, 035501 (2009), [arXiv:0804.4315 \[hep-ph\]](#).
- [34] A. V. Viatkina, D. Antypas, M. G. Kozlov, D. Budker, and V. V. Flambaum, Dependence of atomic parity-violation effects on neutron skins and new physics, *Phys. Rev. C* **100**, 034318 (2019), [arXiv:1903.00123 \[physics.atom-ph\]](#).
- [35] D. Antypas, A. Fabricant, J. E. Stalnaker, K. Tsigutkin, V. V. Flambaum, and D. Budker, Isotopic variation of parity violation in atomic ytterbium, *Nature Phys.* **15**, 120 (2019), [arXiv:1804.05747 \[physics.atom-ph\]](#).

- [36] B. M. Roberts, V. A. Dzuba, and V. V. Flambaum, Parity and time-reversal violation in atomic systems, *Ann. Rev. Nucl. Part. Sci.* **65**, 63 (2015), [arXiv:1412.6644 \[physics.atom-ph\]](#).
- [37] M. S. Safronova, D. Budker, D. DeMille, D. F. J. Kimball, A. Derevianko, and C. W. Clark, Search for new physics with atoms and molecules, *Rev. Mod. Phys.* **90**, 025008 (2018), [arXiv:1710.01833 \[physics.atom-ph\]](#).
- [38] W. J. Marciano and A. Sirlin, Radiative corrections to atomic parity violation, *Phys. Rev. D* **27**, 552 (1983).
- [39] W. J. Marciano and A. I. Sanda, Parity violation in atoms induced by radiative corrections, *Phys. Rev. D* **17**, 3055 (1978).
- [40] W. J. Marciano and A. Sirlin, Some general properties of the  $O(\alpha)$  corrections to parity violation in atoms, *Phys. Rev. D* **29**, 75 (1984).
- [41] P. G. Blunden, W. Melnitchouk, and A. W. Thomas,  $\gamma Z$  box corrections to weak charges of heavy nuclei in atomic parity violation, *Phys. Rev. Lett.* **109**, 262301 (2012).
- [42] B. Duch, P. Masjuan, and H. Spiesberger,  $\gamma Z$  box at low energy (2026), [arXiv:2601.13819 \[hep-ph\]](#).
- [43] S. Navas and et. al., Particle data group, review of particle physics, *Phys. Rev. D* **110**, 030001 (2024).
- [44] J. Erler and A. Freitas, [Electroweak model and constraints on new physics \(pdg 2024 review, section on atomic parity violation\)](#), Particle Data Group online review PDF (2024).
- [45] H. B. Tran Tan, D. Xiao, and A. Derevianko, Reevaluation of stark-induced transition polarizabilities in cesium, *Phys. Rev. A* **108**, 022808 (2023).
- [46] A. A. Vasilyev, I. M. Savukov, M. S. Safronova, and H. G. Berry, Measurement of the  $6s-7p$  transition probabilities in atomic cesium and a revised value for the weak charge  $Q_W$ , *Phys. Rev. A* **66**, 020101 (2002).
- [47] V. A. Dzuba and V. V. Flambaum, Off-diagonal hyperfine interaction and parity nonconservation in cesium, *Phys. Rev. A* **62**, 052101 (2000).
- [48] Z.-l. Zhang, X. Feng, M. Gorchtein, L.-C. Jin, C. Liu, and C.-Y. Seng, Lattice QCD determination of the  $\gamma Z$  box contribution to the proton weak charge (2026), [arXiv:2601.06582 \[hep-lat\]](#).
- [49] Jefferson Lab Qweak Collaboration, Precision measurement of the weak charge of the proton, *Nature* **557**, 207–211 (2018), Proton weak charge  $Q_W^p = 0.0719 \pm 0.0045$ .
- [50] SLAC E158 Collaboration, P. L. Anthony et al., Precision Measurement of the Weak Mixing Angle in Møller Scattering, *Phys. Rev. Lett.* **95**, 081601 (2005), Extracted weak charge of the electron  $Q_W^e = -0.053(11)$ .
- [51] V. A. Dzuba, V. V. Flambaum, and Y. V. Stadnik, Probing low-mass vector bosons with parity nonconservation and nuclear anapole moment measurements in atoms and molecules, *Phys. Rev. Lett.* **119**, 223201 (2017).
- [52] W. J. Marciano and J. L. Rosner, Atomic parity violation as a probe of new physics, *Phys. Rev. Lett.* **65**, 2963 (1990).